ACTA TECHNICA JAURINENSIS
Vol. XX, No. Y, pp. ZZ-ZZ, 2025
10.14513/actatechjaur.00801

Research Article

Comparative Analysis of Surface Topography in Plunge and Face Milling: A Parametric Study into Skewness and Kurtosis

Afraa Khattab[1,*], István Sztankovics[1], Csaba Felhő[1]

[1]Institute of Manufacturing Science, University of Miskolc
H-3515 Miskolc, Hungary
*e-mail: afraa.khattab@student.uni-miskolc.hu

Submitted: 08/06/2025 Revised: 14/08/2025 Accepted: 12/09/2025 Published online: 01/10/2025

Abstract: Optimizing milling procedures to enhance surface quality is crucial in modern manufacturing, where selecting appropriate strategies is paramount for achieving desired surface characteristics in precision-engineered components. This investigation provides a comparative experimental analysis of plunge milling (axial feed) versus face milling (radial feed), specifically evaluating their influence on achievable surface roughness when machining flat surfaces. Key machining parameters—cutting speed, feed per tooth, and depth of cut—were systematically varied for both techniques to quantify how their choice distinctly affects the final surface finish. Experimental results, supported by detailed statistical and graphical interpretation, demonstrated notable differences in surface quality between the two methods across various parameter settings. Consistently, face milling yielded superior surface quality compared to plunge milling under the investigated conditions and across the tested parameter range. The research clarifies the complex interplay and specific relationships between machining parameters and the resultant surface topography for both plunge and face milling. These findings offer practical guidance and valuable insights for optimizing parameter selection and choosing between milling strategies. This enables manufacturers to achieve specific surface roughness targets where surface integrity and finishing are critical quality criteria.

Keywords: Skewness; Kurtosis; Surface Topography; Plunge Milling; Face Milling

I. INTRODUCTION

Surface quality plays a pivotal role in the performance and durability of precision-machined components, influencing factors such as wear resistance, fatigue life, and aesthetic appeal [1-3]. Therefore, achieving optimal surface roughness is fundamental in manufacturing processes across aerospace, automotive, and tooling [4, 5]. Among the array of machining operations, plunge and face milling represent distinct approaches for shaping components, particularly relevant in aerospace and automotive industries where surface integrity is critical [6-10]. While face milling is generally regarded as the preferred method for attaining superior surface finishes, plunge milling offers potential advantages in scenarios such as deep cavity machining or parts with limited access [11-14]. The final texture of a machined surface, quantified by its roughness, is a key determinant of its performance in application [5, 15]. The selection of an appropriate milling strategy—be it plunge or face milling—and its associated parameters, such as cutting speed, feed rate, and depth of cut, profoundly impact the resultant surface roughness [16-20]. Manufacturers striving for superior surface quality often face a complex decision when choosing between these methods, as each presents unique implications for the final surface topography, with inherent advantages and limitations concerning the finish they can produce [11, 21, 22]

Despite extensive research on these techniques, few studies have directly and exclusively compared the impact of plunge and face milling on surface roughness while systematically varying critical machining parameters such as cutting speed, feed per tooth, and depth of cut [2, 7, 14, 23]. While recognized as a promising alternative to conventional milling in specific contexts [7, 24, 25], Plunge milling's impact on surface finish, particularly concerning the formation of step-over marks or scallops and the overall nature of surface generation, remains a key consideration and an area requiring detailed investigation [11, 12, 26-28]. Conversely, face milling is generally preferred, where excellent surface finishes are a primary objective [22, 29-33]. Direct comparative studies with plunge milling,

focusing specifically on surface roughness under varied conditions, are less common [2, 7, 14]. Most existing work evaluates multiple performance metrics—such as cutting forces, tool wear, and material removal rates—alongside surface finish, which complicates isolating the specific influence on surface roughness.

Furthermore, conflicting findings exist regarding whether optimized plunge milling can achieve surface finishes comparable to or better than face milling under certain conditions [34-37]. For example, some studies report significantly higher surface scallop heights for plunge milling than face milling [24], while others suggest that careful parameter optimization can close this gap [2, 7, 14]. While existing research has often focused on average roughness parameters, a deeper understanding of how different milling strategies affect higher-order surface topography characteristics is crucial for predicting functional performance.

This study aims to provide a quantitative comparison between plunge milling and face milling techniques, focusing specifically on higher-order surface texture parameters—skewness (R_{sk}) and kurtosis (R_{ku}). While average roughness (R_a) is widely used, it lacks the sensitivity to capture asymmetry and peak sharpness in surface profiles, which are critical for predicting wear resistance, lubricant retention, load-bearing behavior, and fatigue life. By isolating these second and fourth-order parameters and analyzing their relationship with cutting speed, feed per tooth, and depth of cut under a full factorial experimental design, this research delivers a more nuanced understanding of the surface generation mechanisms in each milling strategy. Achieving this aim enables manufacturers to make more informed decisions when selecting between plunge and face milling, based not only on surface finish but on functional performance. The findings offer practical guidance for optimizing machining parameters to produce tailored surface textures, support predictive modelling of surface behaviour, and expand the potential applications of plunge milling in geometrically constrained or high-integrity components.

II. MATERIAL AND METHOD

This comparative experimental investigation, which analyzed surface roughness, was conducted under meticulously controlled machining conditions. Standardized equipment and a systematic variation of process parameters were employed to ensure the reliability and accuracy of the findings related to surface characteristics across all trials.

Machine tool: All experiments were performed on a Perfect Jet MCV-M8 CNC machining center (Ping Jeng Machinery Industry Co., Ltd, Taichung City, Taiwan) located at the Institute of Manufacturing Science, University of Miskolc, Hungary. This high-precision platform features a BT40 spindle taper, a maximum speed of 10,000 rpm, and a 7.5/11 kW spindle motor, providing excellent stability and adequate power for consistent material removal in both plunge and face milling operations.

Cutting tool and inserts: A unified cutting tool assembly was utilized for both face and plunge milling operations to ensure comparability: a Sandvik Coromant CoroMill 390 end mill (R390-032EH25-17L) coupled with an R390-032EH25-17L tool holder featuring a modular EH25 interface. The cutter, with a 32 mm diameter and a 25 mm arbor size, is designed for 90° shoulder milling, ramping, and plunge operations, as shown in **Fig. 1**. The selection of a single tool suitable for both processes was a deliberate choice to isolate the effects of the milling strategy kinematics, rather than comparing potentially optimized but different tools for each method.

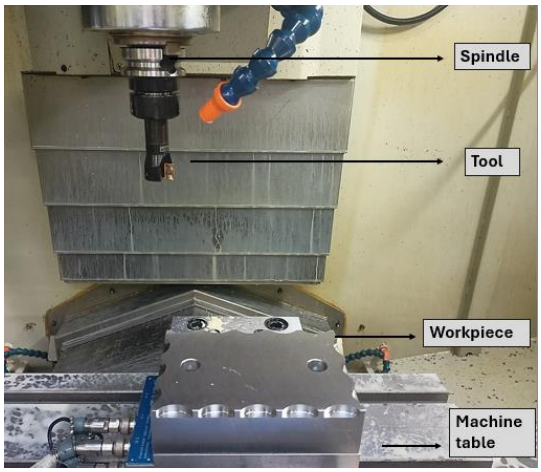

Figure 1. *Experimental setups*

Workpiece material: The workpiece material selected for this study was C45 medium carbon steel, supplied in rectangular blocks measuring 100 mm x 50 mm x 25 mm. This steel grade was chosen for its widespread industrial application and well-documented machinability, providing a relevant basis for surface quality assessment. Typical mechanical and physical properties for C45 steel in its normalized condition include a Brinell hardness of approximately 170-220 HB, a tensile strength of around 620-700 MPa, and a thermal conductivity of about 50 W/(m·K). The chemical composition (wt.%) is nominally: C 0.42-0.50, Mn 0.50-0.80, Si 0.10-0.40, P ≤0.045, S ≤0.045.

Prior to machining, each workpiece was securely fixtured in a precision machine vise. Care was taken to ensure the workpiece was seated correctly and aligned to minimize any potential tilt relative to the machine tool axes. Following machining and before roughness assessment, the workpiece remained fixtured, or was carefully remounted, and its

alignment was visually inspected to ensure no significant tilt that could affect the profilometry readings**.**

This research employed a complete factorial experimental design to systematically examine the effects of three critical machining parameters (cutting speed (v_c), feed per tooth (f_z), and axial depth of cut (a_p) on machining outcomes. The fundamental kinematic differences between the two investigated strategies are critical to understanding the resulting surface topography. **Fig. 2** depicts face milling and plunge milling, defining how the primary machining parameters of feed per tooth (f_z) and axial depth of cut (a_p) were implemented. As shown, in face milling the feed is applied radially across the workpiece, while in plunge milling the feed is applied axially into the workpiece. In addition to these machining parameters, the surface measurement location was included as a key factor in the statistical analysis. This factor, hereafter referred to as 'Direction', consists of two levels: the 'bottom surface' (the bottom of the machined scallop) and the 'Side surface' (the wall of the machined scallop) as shown in **Fig. 3**.

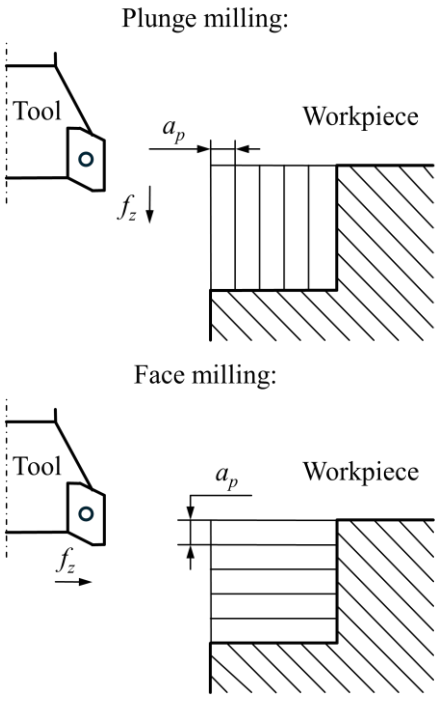

Figure 2. *The kinematic differences between face milling and plunge milling*

Each variable was tested at two levels, as shown in Table 1, to assess individual and combined influences on cutting forces and surface finish. The two-level factorial design was chosen for its ability to systematically examine the main effects of three critical machining parameters and two-way interactions with a reduced number of trials. **Fig. 4** provides a schematic representation of this 2^3 full factorial design, illustrating the eight unique experimental conditions as vertices of a cube defined by the two levels of each of the three factors. The axes represent the three machining parameters: axial depth of cut (a_p), feed per tooth (f_z), and cutting speed (v_c), each at two levels. The eight vertices of the cube correspond to the unique experimental conditions detailed in **Table 1**.

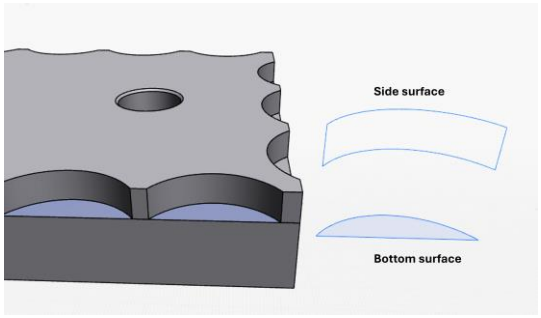

Figure 3. *Schematic of a machined scallop identifying the two distinct areas for surface roughness analysis: the bottom surface and the Side surface.*

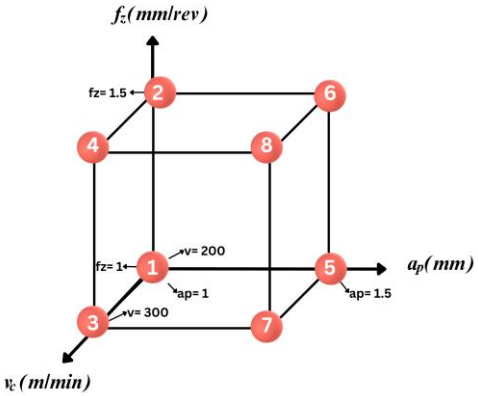

Figure 4. *Schematic of the full factorial experimental design.*

Table 1. *Machining parameter settings for each experimental setup.*

Sample	a_p ***mm***	v_c ***m/min***	f_z ***mm/rev***
1	1	200	0.1
2	1	200	0.15
3	1	300	0.1
4	1	300	0.15
5	1.5	200	0.1
6	1.5	200	0.15
7	1.5	300	0.1
8	1.5	300	0.15

It is important to note that each of these eight conditions represents a single, distinct machining trial; no replicate machining trials were conducted for the main experimental matrix. A single rectangular workpiece block was utilized. On each block,

separate areas were designated for plunge milling and face milling operations, allowing both methods to be tested under the same specific parameter combination (v_c, f_z, a_p) on the same piece of material. Therefore, for each of the eight conditions, one area was subjected to plunge milling, and a different location was subjected to face milling. Fresh cutting inserts were used for each of the eight experimental conditions to ensure consistency across these paired operations.

Roughness measurement: After machining, surface roughness was assessed by the AltiSurf 520 3D topography system with a confocal chromatic probe. Measurements were taken along three generatrix lines on each cylindrical surface to ensure a representative surface quality evaluation. During testing, each scallop had two distinct surfaces—at the pocket bottom and along the side wall. Due to their different geometries and cutting conditions, surface roughness was measured separately in each area.

III. RESULT

Key roughness parameters, (R_{sk} (skewness, **Table 2**), R_{ku}(kurtosis), **Table 3**), were measured across all experimental conditions to evaluate and compare the surface quality resulting from milling methods. The roughness parameters were selected for detailed analysis due to their relevance in characterizing surface profile geometry, sharpness, and asymmetry. Each parameter contributes distinct information to the surface profile assessment [38]:

Table 2. *Surface roughness parameter settings (R_{sk} (μm))*

		Plunge milling				***Face milling***			
Type	***Sample***	***1***	***2***	***3***	***Mean***	***1***	***2***	***3***	***Mean***
Side surface	1	0.164	0.19	0.18	0.177	0.44	0.424	0.277	0.380
	2	-0.193	0.25	0.075	0.044	-0.034	0.061	-0.115	-0.029
	3	0.149	0.026	0.133	0.103	0.043	-0.219	-0.127	-0.101
	4	-0.21	0.26	0.117	0.056	-0.016	-0.274	0.234	-0.019
	5	0.032	-0.018	0.351	0.122	-0.091	0.134	0.067	0.037
	6	-0.137	0.288	0.05	0.067	0.245	0.179	0.35	0.258
	7	0.072	0.086	0.12	0.093	-0.035	0.238	0.278	0.160
	8	0.078	0.054	0.27	0.134	0.056	0.356	-0.169	0.081
Bottom surface	1	0.003	0.188	-0.175	0.005	-0.128	-0.317	-0.303	-0.249
	2	0.199	0.212	0.076	0.162	-0.181	0.02	-0.056	-0.072
	3	0.144	0.246	0.303	0.231	-0.418	-0.657	-0.343	-0.473
	4	-0.045	-0.108	-0.212	-0.122	-0.26	-0.339	-0.188	-0.262
	5	0.12	0.125	0.125	0.123	0.088	-0.018	-0.407	-0.112
	6	-0.108	-0.061	-0.043	-0.071	-0.018	0.009	-0.295	-0.101
	7	0.42	-0.001	-0.042	0.126	-0.236	-0.62	-0.488	-0.448
	8	0.062	-0.231	-0.115	-0.095	-0.281	-0.421	-0.246	-0.316

Table 3. *Surface roughness parameter settings (R_{ku} (μm))*

		Plunge milling				***Face milling***			
Type	***Sample***	***1***	***2***	***3***	***Mean***	***1***	***2***	***3***	***Mean***
Side surface	1	3.28	3.11	3.359	3.250	3.292	3.407	3.267	3.322
	2	2.66	3.577	2.864	3.034	2.595	3.233	2.86	2.896
	3	2.79	2.664	2.833	2.762	2.825	2.696	3.168	2.896
	4	2.783	3.08	2.811	2.891	2.832	2.758	3.449	3.013
	5	2.791	2.767	3.553	3.037	3.149	3.791	3.301	3.414
	6	3.045	4.094	3.064	3.401	3.135	2.781	2.789	2.902
	7	3.107	2.561	2.675	2.781	2.876	2.685	2.595	2.719
	8	2.799	2.625	3.244	2.889	2.911	2.794	2.515	2.740
Bottom surface	1	2.91	2.279	2.51	2.566	3.838	3.657	2.89	3.462
	2	2.734	2.961	3.079	2.925	3.306	3.532	3.39	3.409
	3	3.013	2.889	3.017	2.973	3.362	3.997	3.201	3.520
	4	3.726	3.482	3.705	3.638	3.494	3.64	3.364	3.499
	5	2.81	3.027	2.825	2.887	2.631	2.812	3.718	3.054
	6	2.674	2.814	2.934	2.807	2.615	3.205	3.306	3.042
	7	3.219	3.638	2.683	3.180	3.611	4.613	4.035	4.086
	8	3.832	3.628	2.951	3.470	3.236	3.666	3.422	3.441

R_{sk} (skewness) quantifies the asymmetry of the surface profile. A negative R_{sk}. A positive value suggests a peak-dominated surface, while a negative value indicates a valley-dominated surface, which helps predict lubricant retention or stress concentration.

R_{ku}(kurtosis) reflects the sharpness or flatness of the surface distribution. High R_{ku} values indicate spiky surface features, whereas lower values denote flatter, plateau-like surfaces, which are relevant for understanding fatigue performance and load-bearing capacity.

1. Surface Topography

The interaction between the cutting tool and the confined geometry significantly affects roughness characteristics, leading to distinct trends in R_{sk}, and R_{ku}. To better understand the influence of milling strategy, measure location, and cutting speed on surface roughness parameters, 3D surface plots (**Figs 5-12**) were generated using Origin 2025 software. The presented 3D surface plots illustrate the influence of cutting speed (v_c) and feed per revolution (f_z) on key surface roughness parameters – skewness (R_{sk}), and kurtosis (R_{ku}) – generated surfaces all at a constant axial depth of cut (a_p=1 and 1.5 mm).

A. Influence of Machining Parameters on Skewness (R_{sk})

Skewness (R_{sk}) describes the asymmetry of the surface profile height distribution. A positive R_{sk} indicates a surface dominated by peaks, while a negative R_{sk} suggests a surface dominated by valleys. A striking distinction was observed between plunge and face milling for side surfaces.

Side surfaces: A striking and consistent distinction in R_{sk} behavior was observed between plunge and face milling for side surfaces, with the depth of cut (a_p) modulating the magnitude of these effects.

Plunge milling (**Fig. 5a and 6a**): Consistently generated side surfaces with negative R_{sk} values. At a_p=1 mm (**Fig. 5a**), R_{sk} ranged from approximately -0.04 to -0.17 µm. Increasing $a_p$to 1.5 mm (**Fig. 6a**) resulted in slightly less negative R_{sk} values, ranging from approximately -0.06 to -0.13 µm. For both depths of cut, R_{sk} generally became more negative (more valley-rich) with increasing cutting speed (v_c),

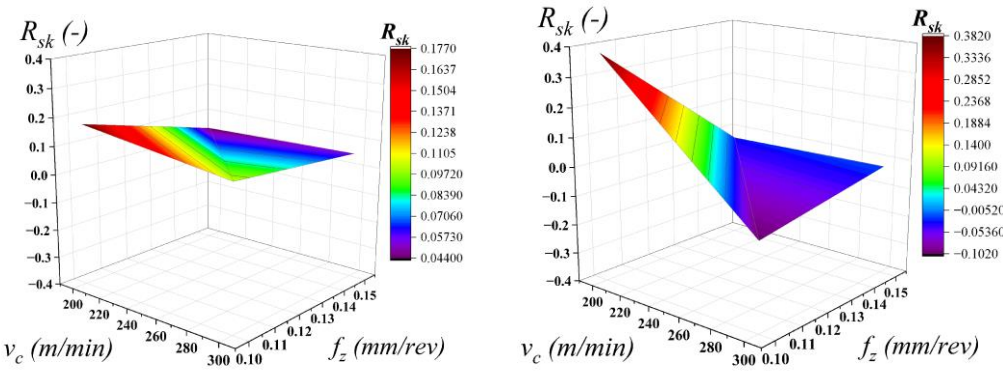

(a) (b)

***Figure 5**. 3D Surface Plot of surface roughness R_{sk} on the side surfaces where the depth of cut a=1 mm (a) plunge milling, (b) face milling*

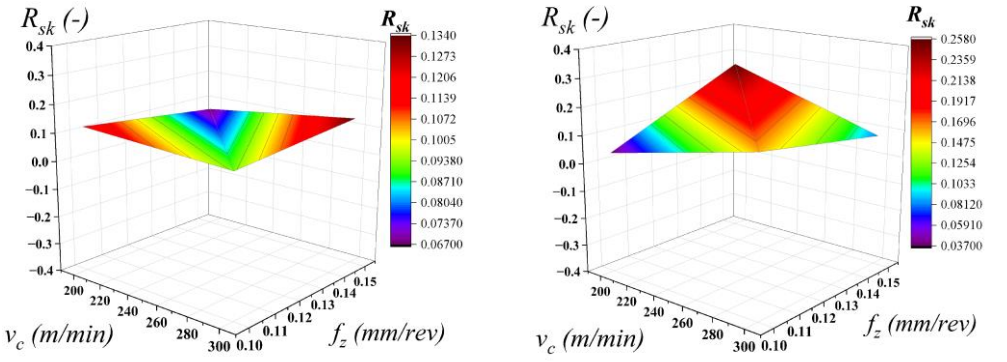

(a) (b)

***Figure 6.** 3D Surface Plot of surface roughness R_{sk} on the side surfaces when the depth of cut a_p=1.5 mm (a) plunge milling, (b) face milling.*

while the influence of feed (f_z) was less pronounced, though higher $f_z$tended to decrease slightly R_{sk}. In face milling (**Fig. 5b and 6b**), conversely, consistently produced side surfaces with positive R_{sk}values. At a_p=1 mm.

R_{sk} ranged from approximately -0.1 (at very low v_c/f_z) to +0.38 µm. When $a_p$was increased to 1.5 mm (**Fig. 6b**), the R_{sk} values became less favourable, ranging from approximately +0.03 to +0.25 µm. For both depths of cut, R_{sk} generally became more positive (more peak-rich) with increasing v_c, with f_z having a secondary, slightly positive influence.

The opposing R_{sk} trends for side surfaces highlight fundamental differences in material removal. Plunge milling's axial engagement likely promotes material tearing, creating valley-dominant textures. Face milling's peripheral cutting on the side wall might lead to material smearing or upward flow, resulting in peak-dominant surfaces. Increasing $a_p$appears to moderate these characteristics R_{sk}values, bringing them closer to zero for both strategies, possibly due to more stable cutting or altered material side-flow.

Bottom surfaces: The influence of the depth of cut a_p on the skeweness R_{sk} for bottom surfaces was also evident, though the overall differed from side surfaces.

Plunge milling (**Fig. 7 and 8**): For bottom surfaces, R_{sk}exhibited a transition. At a_p=1 mm (**Fig. 7a**), R_{sk}decreased from positive values (+0.23 µm) at low v_c/f_z to negative values (-0.12 µm) at high v_c/f_z. A similar, though less pronounced, trend and slightly less negative overall values (i.e., R_{sk}values closer to zero or slightly more positive) were observed when $a_p$was increased to 1.5 mm (Figure 8a), with R_{sk} ranging from approximately +0.12 to -0.09 µm. While in face milling (**Fig. 7b and 8b**), consistently produced bottom surfaces with negative R_{sk}values. a_p=1 mm (**Fig. 7b**), R_{sk}became more negative with increasing v_c and, to a lesser extent, with increasing f_z, ranging from approximately -0.07 to -0.47 µm. Increasing $a_p$to 1.5 mm (**Fig. 8b**) resulted in

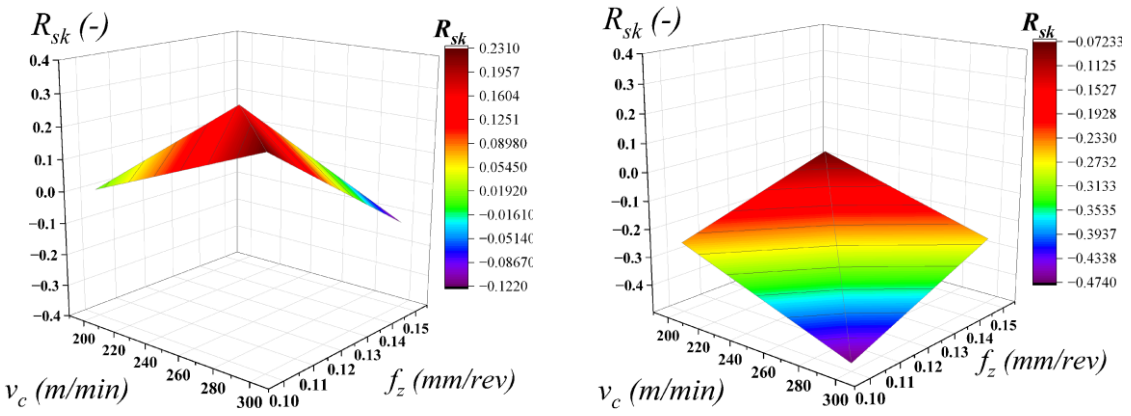

(a) (b)

Figure 7. *3D Surface Plot of surface roughness R_{sk}on the bottom surfaces when the depth of cut a=1 mm (a) plunge milling, (b) face milling.*

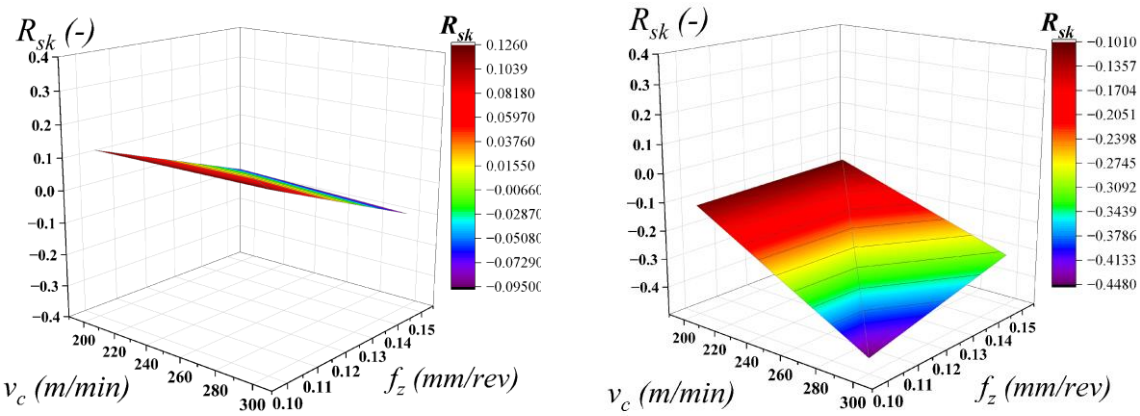

(a) (b)

Figure 8. *3D Surface Plot of surface roughness R_{sk}on the bottom surfaces when the depth of cut a_p=1.5 mm (a) plunge milling, (b) face milling.*

generally less negative R_{sk} values (ranging from approximately -0.10 to -0.44 µm), though the trend of becoming more negative with higher v_c and f_z persisted. For bottom surfaces, both strategies tend towards more valley-rich textures (negative R_{sk}) at higher v_c and f_z. Increasing $a_p$generally resulted in slightly less negative

(or more positive, in the case of plunge milling at low parameters) R_{sk}values, suggesting a moderating effect on valley dominance.

B. Influence of Machining Parameters on Kurtosis (R_{ku})

Kurtosis (R_{ku}) describes the peakedness of the surface profile. $R_{ku} \approx 3$ indicates a mesokurtic distribution; $R_{ku} > 3$ is leptokurtic (spiky); $R_{ku} < 3$ is platykurtic (flatter).

Side surfaces: The kurtosis of side surfaces showed relatively consistent behavior across milling strategies and depths of cut. Plunge milling (**Fig. 9a and 10a**), Generally yielded R_{ku} values slightly below or around 3. At a_p=1 mm (**Fig. 9a**), R_{ku} ranged from approximately 2.7 to 3.3. Increasing a_p to 1.5 mm (**Fig. 10a**) resulted in marginally higher R_{ku} values, ranging from approximately 2.7 to 3.4. For both depths of cut, R_{ku} tended to decrease slightly with increasing v_c and f_z, suggesting a shift towards a more platykurtic surface. Face milling (**Fig. 9b and 10b**), Showed similar R_{ku} values and trends. At a_p=1 mm R_{ku} was- approximately 2.8 to 3.3 (**Fig. 9b**). With a_p increased 1.5 mm (**Fig. 10b**), to R_{ku} values were also marginally higher, ranging from approximately 2.7 to 3.4. Again, for both depths of cut, R_{ku} tended to decrease slightly with increasing v_c and f_z. Overall, for side surfaces, R_{ku} values remained near mesokurtic, with higher v_c and $f_z$promoting slightly flatter distributions. Increasing a_p had a minimal effect, slightly raising R_{ku} values for both milling types.

Bottom surfaces: The behavior of R_{ku} on the bottom surfaces showed more pronounced differences, especially concerning the interaction with a_p Plunge milling (**Fig. 10),** Showed R_{ku} values generally increase with both v_c and f_z. At a_p =1 mm (**Fig. 11a)** R_{ku} ranged from approximately 2.5 (platykurtic) to 3.6 (slightly leptokurtic). When a_p increased to 1.5 mm (**Fig. 12a**), the overall R_{ku} values were slightly lower, ranging from

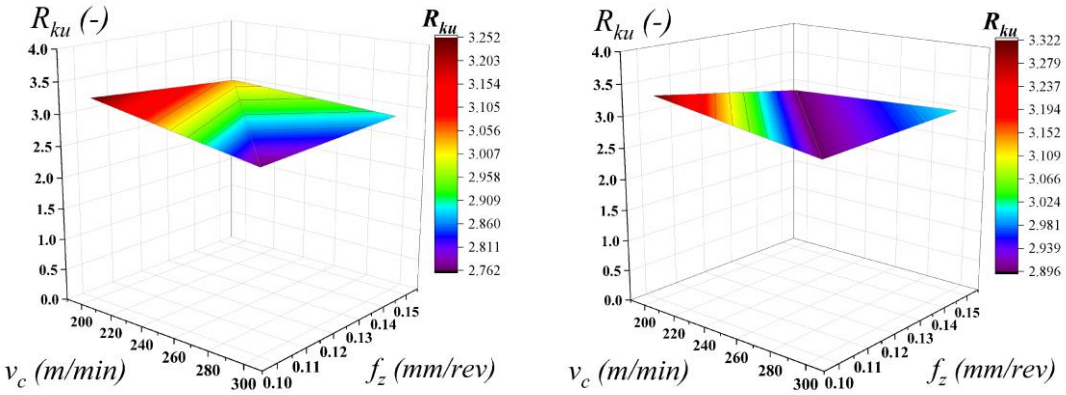

(a) (b)

Figure 9. *3D Surface Plot of surface roughness R_{ku} on the side where the depth of cut a=1 mm (a) plunge milling, (b) face milling.*

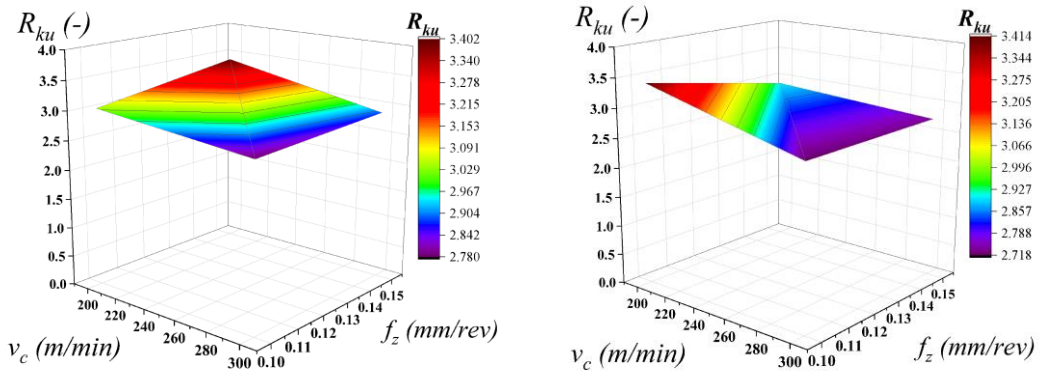

(a) (b)

Figure 10. *3D Surface Plot of surface roughness R_{ku} on the side when the depth of cut a=1.5 mm (a) plunge milling, (b) face milling.*

approximately 2.8 to 3.4, but the increasing trend with v_c and f_z remained. Face milling (**Fig. 11b and 12b**), Also showed R_{ku} on the bottom surfaces, increasing with v_c and f_z. Strikingly, increasing a_p to 1.5 mm (**Fig. 12b**) significantly- amplified this effect, with R_{ku} ranging. At a_p =1 mm (**Fig. 11b**), R_{ku} values were relatively high and stable (approximately 3.4-3.5), indicating a consistently somewhat spiky (leptokurtic) surface. from approximately 3.0 to 4.0, indicating a transition to more distinctly leptokurtic (spiky) surfaces, particularly at higher v_c and f_z. Thus, for bottom surfaces, increasing a_p had opposing effects on R_{ku} depending on the milling strategy, it slightly R_{ku} for plunge milling while significantly increasing it (making surfaces spikier) for face milling.

IV. Discussion

The experimental results presented in Chapter III reveal statistically significant and functionally relevant differences in the surface topography generated by plunge and face milling. A detailed examination of the surface skewness (R_{sk}) and kurtosis (R_{ku}) provides insight into the distinct material removal mechanisms at play. The observed differences in R_{sk} and R_{ku} stem primarily from the kinematic engagement between the- cutting tool and workpiece in each milling strategy. In plunge milling, the axial tool engagement tends to tear material and create surface valleys, which leads to more negative effects. R_{sk} values (valley-dominant surfaces) and slightly flatter profiles (lower R_{ku}). Conversely, face milling, which engages the material radially and uses peripheral cutter motion, creates smoother surface transitions and often results in peak dominant profiles dominant profiles (positive R_{sk}) and sharper features (higher Rku). These outcomes are also influenced by how chip thickness and uncut material accumulate in each strategy. Face milling has more uniform chip formation and better flushing of material, contributing to reduced surface randomness and elevated R_{ku}.

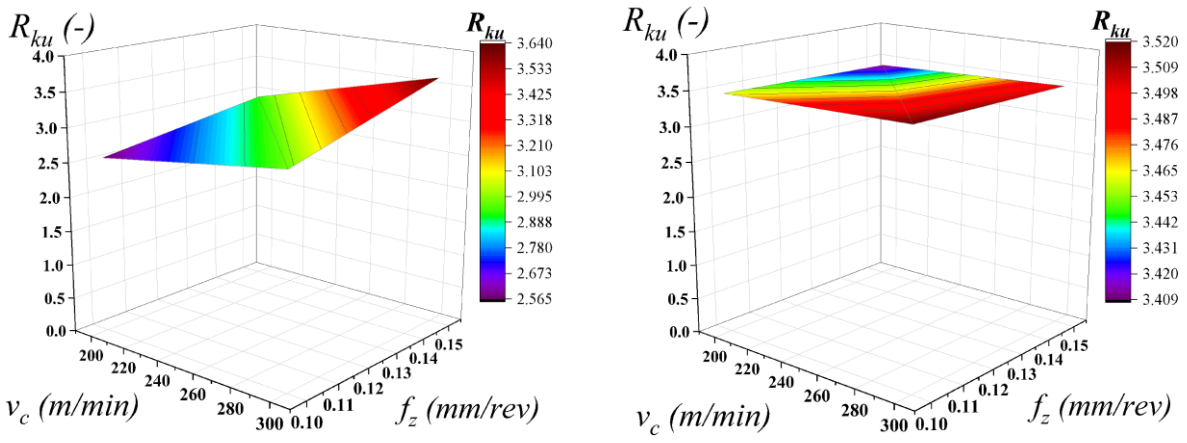

(a) (b)

Figure 11. *3D Surface Plot of surface roughness R_{ku} on the bottom surfaces when the depth of cut a=1 mm (a) plunge milling, (b) face milling.*

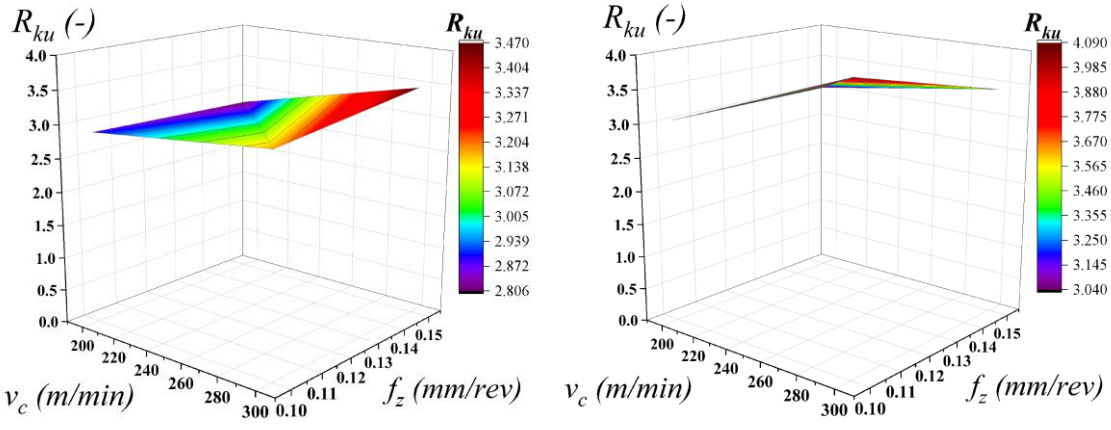

(a) (b)

Figure 12. *3D Surface Plot of surface roughness R_{ku} on the bottom surfaces when the depth of cut a=1.5 mm (a) plunge milling, (b) face milling.*

1. Statistical analysis

Surface roughness was assessed using quantitative parameters measured at two locations on the machined pockets. All statistical analyses were performed using IBM SPSS Statistics. Prior to conducting inferential tests, the underlying assumptions of normality and- homogeneity of variance was rigorously evaluated. Prior to conducting inferential tests, the underlying assumptions of normality and homogeneity of variance were rigorously evaluated. The Shapiro–Wilk test confirmed that the distribution of all variables did not significantly deviate from normality ($p > 0.05$), while Levene's test verified the equality of variances across groups. These diagnostic checks validated the appropriateness of employing parametric methods. The subsequent analysis focused on assessing the main and interaction effects of the selected factors on surface topography parameters, in direct alignment with the study's core objective of elucidating process-structure relationships in machining operations.

A two-way ANOVA was performed to determine the statistical significance of Milling Type (plunge vs. face) and Measurement Direction (bottom vs. side surface), as well as their interaction. The ANOVA results for the R_{sk} parameter in **Table 4** revealed significant main effects of machining measurement direction _($F(1, 28) = 19.932$, $p < 0.001$) and milling type ($F(1, 28) = 10.311$, $p = 0.003$), along with a significant interaction between them ($F(1, 28) = 10.805$, $p = 0.003$). These findings indicate that both factors independently and jointly influence surface skewness. The model accounted for 59.4% of the variance in R_{sk} (adjusted $R^2 = 0.551$), with high observed power values (>0.87), confirming the robustness of the results. Thus, optimizing R_{sk} requires simultaneous consideration of machining direction and milling strategy.

While the ANOVA results for the R_{ku} parameter in **Table 5** indicated a statistically significant main effect of machining direction ($F(1, 28) = 4.420$, $p = 0.045$), suggesting that surface kurtosis is influenced by tool orientation. However, the effect of milling type ($F(1, 28) = 3.741$, $p = 0.063$) and its interaction with direction ($F(1, 28) = 2.677$, $p = 0.113$) were not statistically significant at the $\alpha = 0.05$ level.

Furthermore, data analysis was employed utilizing box plots. The subsequent section presents an account of the statistical outcomes derived from these procedures. In terms of skewness (R_{sk}, **Fig. 13**), face milling produced negatively skewed surfaces (median ≈ –0.2, IQR: –0.3 to 0.0), suggesting a dominance of valleys favorable for lubricant retention. In contrast, plunge milling yielded positively skewed surfaces (median ≈ 0.1, IQR: 0.05–0.15), indicating peak dominated profiles that may be prone to higher initial wear. To assess the consistency of these skewness values, the coefficient of variation (CV) was considered. However, given that the overall mean R_{sk} values for both milling strategies are very close to zero (Face: -0.076; Plunge: 0.072), the standard CV calculation (SD/|Mean| * 100%) can yield disproportionately large and potentially misleading percentages. For face milling, the calculated CV was approximately 314.01%, and for plunge milling, it was approximately 137.92%. Due to theinfluence of near-zero means on the CV, it is more informative in this instance to directly compare the standard deviations (SD) as a measure of absolute dispersion. The standard deviation for R_{sk} values from face milling were 0.238, while for plunge milling, it was 0.100. This indicates that the R_{sk} values generated by face milling exhibited a wider absolute spread (greater variability) around their near-zero mean compared to those from plunge milling under the investigated conditions. While plunge milling's R_{sk} values were also variable, and

Table 4. *Two-way ANOVA tests result for R_{sk}*

Source	*df*	*Mean Square*	*F*	*Sig. (p-value)*	*Partial η²*	*Observed Power*
Direction	1	0.338	19.932	< 0.001	0.416	0.991
Milling Type	1	0.175	10.311	0.003	0.269	0.873
Direction × Milling Type	1	0.183	10.805	0.003	0.278	0.887
Corrected Model (R² = 0.594)	3	0.232	13.683	< 0.001	—	1.000

Table 5. *Two-way ANOVA tests result for R_{ku}*

Source	*df*	*Mean Square*	*F*	*Sig.(p-value)*	*Partial η²*	*Observed power*
Direction	1	0.408	4.420	0.045	0.136	0.528
Milling Type	1	0.345	3.741	0.063	0.118	0.463
Direction × Milling Type	1	0.247	2.677	0.113	0.087	0.352
Corrected Model (R² = 0.594)	3	0.333	3.613	0.025	—	0.733

their absolute dispersion was considerably smaller. This suggests that while both methods produce R_{sk} values that fluctuate around zero, the magnitude of this fluctuation was less for plunge milling.

For the surface kurtosis (R_{ku}), the ANOVA results in **Table 5** indicated a statistically significant main effect of machining direction (F(1, 28) = 4.420, p = 0.045). However, it is critical to note that the overall model demonstrated a low goodness of fit, explaining only - 27.9% of the variance in R_{ku} (adjusted R^2 = 0.202). This low R^2 value suggests that while 'Direction' has a statistically identifiable effect, its practical significance is limited, and the model has weak predictive power for surface kurtosis. The effects of milling type (p = 0.063) and its interaction (p = 0.113) were not statistically significant. The observed power for the 'direction' factor was moderate (0.528). In contrast, the statistical power for 'milling type' and its interaction with direction remained low. This low power indicates that the experiment may have had insufficient sensitivity to detect an actual effect for these factors if one existed. Therefore, while the p-values for milling type (p = 0.063) and the interaction (p = 0.113) were not statistically significant, we cannot definitively conclude that they do not affect surface kurtosis. A future study with a larger sample size would be needed to explore this potential relationship more conclusively. These findings highlight the directional dependency of R_{ku}. However, further investigation is warranted to clarify the role of milling strategies and their effects on interaction.

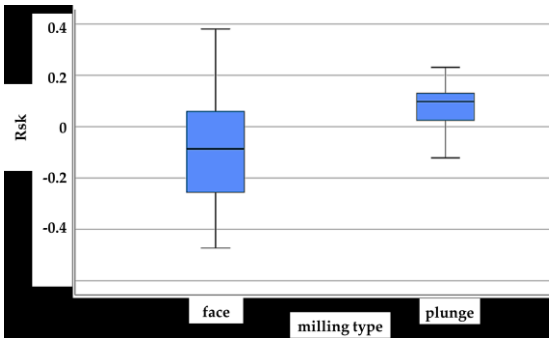

Figure 13. *Boxplots of Surface Roughness R_{sk}*

The analysis of surface kurtosis (R_{ku}) in **Fig. 14** revealed that face milling consistently produced higher kurtosis values (median ≈ 3.2, IQR: 2.9–3.45) compared to plunge milling (median ≈ 2.95, IQR: 2.8–3.2). This indicates that face milling tends to generate leptokurtic profiles with sharper peaks and valleys (R_{ku} > 3), whereas plunge milling results in platykurtic profiles characterized by more rounded or flattened surface features (R_{ku} < 3).To assess the predictability or consistency of these kurtosis values across the varied machining parameters, the coefficient of variation (CV) was calculated based on the mean R_{ku} values for each milling strategy (data from Table 3).

Plunge milling exhibited a CV for R_{ku} of approximately 9.50%, while face milling showed a CV of roughly 11.26%. A lower CV signifies less relative variability and thus greater consistency. Therefore, these results suggest that while face milling produced, on average, higher R_{ku} values, plunge milling generated R_{ku} values with slightly greater relative consistency (i.e., were more predictable relative to their mean) across the range of cutting speeds, feeds, and depths of cut investigated in this study. This nuanced finding highlights that the choice of milling strategy impacts not only the average topographical characteristics but also their variability under different process conditions. The selection of machining strategy should, therefore, be guided by the functional requirements of the surface, such as lubrication efficiency or wear resistance.

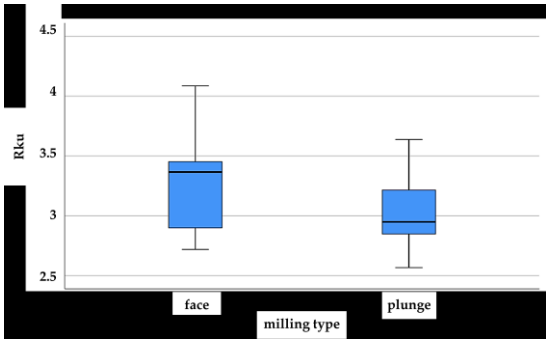

Figure 14. *Boxplots of Surface Roughness R_{ku}*

2. Surface Texture Characteristics (R_{sk} and R_{ku})

Characterizing machined surfaces is critical for predicting and ensuring the functional performance of manufactured components. Average roughness parameters provide a general indication of surface height variations, while Higher-order statistical parameters, such as skewness (R_{sk}) and kurtosis (R_{ku}) offer more detailed insights. Skewness (R_{sk}) quantifies the asymmetry of the surface height distribution; a negative R_{sk} indicates a predominance of plateaus or bearing surfaces, while a positive R_{sk} suggests a surface dominated by deep valleys. Kurtosis (R_{ku}) describes the peakedness or sharpness of the height distribution; R_{ku}> 3 indicates a spiky (leptokurtic) profile, R_{ku}< 3 a bumpy or flat (platykurtic) profile and R_{ku}≈ 3 suggests a Gaussian distribution. The following plots (**Fig. 15 and Fig. 16**) present an analysis of R_{sk} versus R_{ku} for surfaces generated by plunge milling and face milling operations.

These plots elucidate the distinct topographical signatures produced by each milling process and investigate the influence of varying cutting

parameters— depth of cut (a_p), cutting speed (v_c), and feed per tooth (f_z)_on these surface texture attributes. The data points within the (R_{sk}-R_{ku}Plots are coded according to the specific machining parameters employed, as follows:

- Shape of marker (depth of cut, a_p): while a square represents a depth of cut, a_p = 1 mm. The triangle is for a depth of cut a_p = 1.5 mm.
- Color of marker (cutting speed, v_c): the red indicates a cutting speed, v_c= 200 m/min. Blue is for v_c= 300 m/min.
- Size of marker (feed per tooth, f_z): the small marker corresponds to a feed per tooth f_z= 0.1 mm/rev. A significant marker related to a feed per tooth, f_z= 0.15 mm/rev.

On the side surfaces generated by plunge milling, increasing the depth of the cut a_p(to 1.5 mm) generally promoted more negative R_{sk}values, indicative of enhanced plateau formation. Similarly, higher cutting speeds (300 m/min) tended to yield more negatively skewed profiles. R_{ku} values remained remarkably consistent and near-Gaussian (R_{ku}≈ 3) across these parameter changes.

The effect of increased feed per tooth was notably interactive: when combined with a lower speed and depth of cut (v_c=200 m/min, a_p=1mm), it shifted R_{sk}towards positive values under conditions of higher speed and depth of cut (v_c=300 m/min, a_p=1.5mm), increased feed f_z led to more negative R_{sk} values.

Face-milled side surfaces exhibited the most incredible sensitivity and the widest dispersion in space- of R_{sk}-R_{ku}. An increased depth of cut a_p (to 1.5 mm), particularly when combined with a lower cutting speed (200 m/min), could shift R_{sk} from negative to significantly positive values, indicating a transition from plateau-dominant to valley-dominant topographies. Conversely, higher cutting speeds (300 m/min) consistently favored negatively skewed side surfaces. R_{ku} values also showed considerable scatter, influenced by the interplay of parameters. The most pronounced effect of the feed was observed

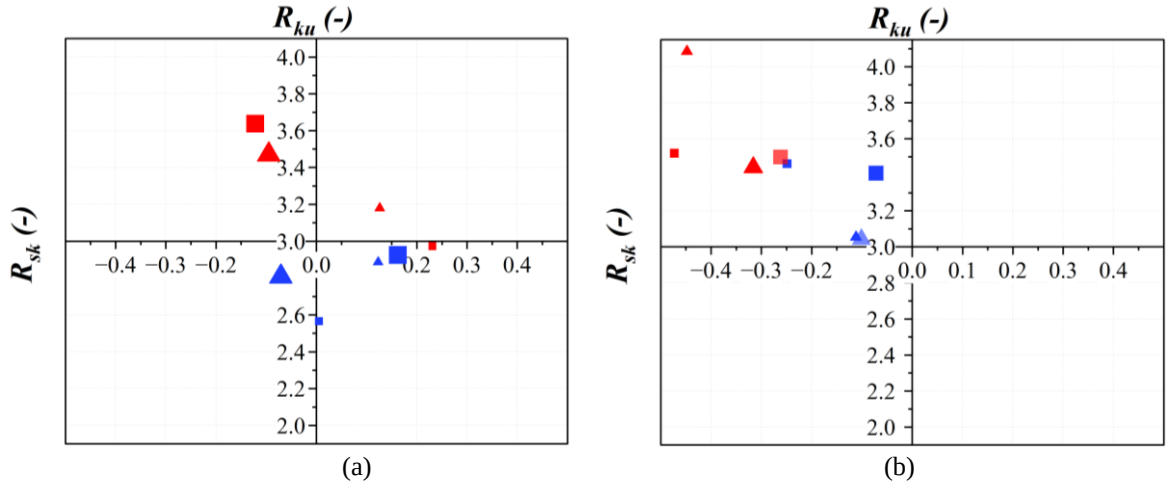

Figure 15. *Skewness (R_{sk}) versus kurtosis (R_{ku}) for bottom measured surfaces under varied machining conditions(a) plunge milling, (b)face milling.*

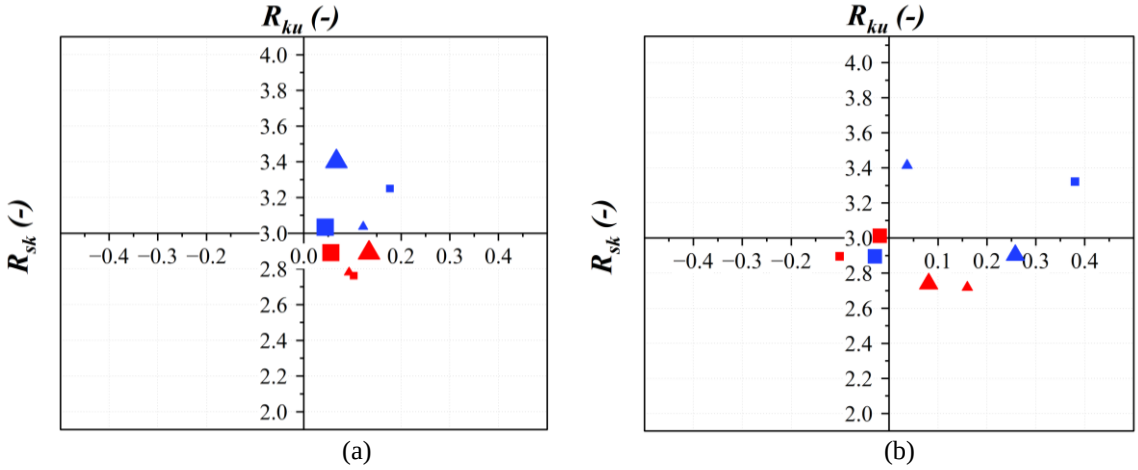

Figure 16. *Skewness (R_{sk}) versus kurtosis (R_{ku}) for side measured surfaces under varied machining conditions(a) plunge milling, (b)face milling.*

under specific conditions: an increased feed. f_z (to 0.15 mm/rev) at low.

For plunge-milled bottom surfaces, an increase in the depth of the cut a_p (from 1 mm to 1.5 mm) generally tended to produce more negative R_{sk}values, indicative of more pronounced plateau structures, alongside a modest increase in R_{ku}, suggesting slightly spikier profiles. Conversely, elevated cutting speeds (from 200 to 300 m/min) typically resulted in R_{sk}values closer to zero and marginally lower R_{ku}values, potentially yielding flatter profiles. The influence of an increased - feed per tooth f_z (from 0.1 to 0.15 mm/rev) was less distinct, exhibiting variable effects on R_{sk} and R_{ku}.

In contrast, for face-milled bottom surfaces, an increased depth of cut a_p (from 1 mm to 1.5 mm) markedly elevated R_{ku} values, signifying substantially spikier profiles. Higher cutting speeds (300 m/min compared to 200 m/min) also increased. R_{ku}, particularly at the greater depth of cut a_p (1.5 mm) and could slightly enhance negative skewness. The impact of increased feed per tooth f_z was less pronounced on these bottom surfaces compared to the dominant effects of depth of cut and cutting speed.

V. CONCLUSION

This comparative experimental investigation has systematically elucidated the distinct effects of plunge milling and face milling strategies, along with key machining parameters (cutting speed, v_c=; feed per revolution, f_z; and depth of cut a_p), on the resulting surface skewness (R_{sk}) and kurtosis (R_{ku}). The findings reveal complex, often interacting, relationships that significantly influence the final surface topography. A fundamental distinction was observed in skewness (R_{sk}) on side surfaces: plunge milling consistently produced negative R_{sk} values (valley-dominant), while face milling invariably yielded positive R_{sk} values (peak-dominant), with increasing a_p generally moderating these characteristics. On the bottom surfaces, both strategies tended toward negative R_{sk} at higher parameters, with a_p again showing a moderating effect. Regarding kurtosis (R_{ku}), side surfaces exhibited similar near-mesokurtic profiles for both milling types. In contrast, the bottom surface R_{sk} showed more pronounced differentiation, notably increasing a_p slightly decreased R_{sk} for plunge milling, but significantly increased R_{sk} for face milling, resulting in markedly spikier bottom surfaces for the latter. Furthermore, an analysis of the consistency of these topographical parameters revealed essential distinctions. For surface kurtosis (R_{ku}), plunge milling demonstrated slightly greater relative consistency (CV ≈ 9.50%) across the tested parameter range compared to face milling (CV ≈ 11.26%). Regarding surface skewness (R_{sk}), while both methods produced values fluctuating around a near-zero mean, a direct comparison of standard deviations indicated that plunge milling (SD = 0.100) resulted in considerably less absolute dispersion than face milling (SD = 0.238), suggesting more contained R_{sk} outcomes for plunge milling under the investigated conditions.

These results underscore that the choice of milling strategy and the careful selection of cutting parameters are critical not only for achieving target average topographical characteristics but also for ensuring the predictability of these features. Such insights are vital for tailoring specific surface textures with direct implications for functional performance, such as lubrication, wear, and contact mechanics. While these findings provide valuable guidance, future research could expand upon this by investigating a wider range of materials, tool geometries, and correlating these higher-order parameters with direct functional testing.

While these findings provide valuable insights, the investigation used a fixed tool diameter and a single workpiece material (C45 steel). This limitation may restrict the broader applicability of the results and highlight opportunities for future research. Subsequent studies should build on this foundation by incorporating various tool geometries, a wider range of workpiece materials, and an expanded set of cutting parameters. Future research should establish direct correlations between the measured R_{sk} and R_{ku} values and other functional surface roughness parameters, beyond just cutting forces, to develop a more comprehensive understanding of surface characteristics. These insights are expected to be a foundation for creating more sophisticated predictive models for both plunge and face milling processes.

AUTHOR CONTRIBUTIONS

A. Khattab: Experiments, Theoretical analysis, Investigation, Visualization, Writing—original draft preparation, Writing—review and editing.

I. Sztankovics: Conceptualization, Experiments, Theoretical analysis, Writing—review and editing.

Cs. Felhő: Conceptualization, Theoretical analysis, Project administration, Writing—review and editing.

DISCLOSURE STATEMENT

The authors declare that they have no known competing financial interests or personal relationships that could have appeared to influence the work reported in this paper.

REFERENCES

[1] D. C. Chen and T. W. Chen, 'Surface roughness analysis of high speed milling in grooving', *J. Phys.: Conf. Ser.* 2020 (1) (2021) p. 012034. https://doi.org/10.1088/1742-6596/2020/1/012034

[2] G. Gómez *et al.*, 'Comparison between milling roughing operations in full slotting manufacturing: trochoidal, plunge and conventional milling', *IOP Conf. Ser.: Mater. Sci. Eng.* 1193 (1) (2021) p. 012003. https://doi.org/10.1088/1757-899X/1193/1/012003

[3] H. Xin, Y. Shi, and T. Zhao, 'Compound efficient and powerful milling machine tool of blisk', *Int J Adv Manuf Technol* 98 (5–8) (2018) pp. 1745–1753. https://doi.org/10.1007/s00170-018-2225-1

[4] C. Chen, C. Wu, T. Zhang, and S. Y. Liang, '3D curved surface milling modeling for the topography simulation and surface roughness prediction', *Journal of Manufacturing Processes* 137 (2025) pp. 150–165. https://doi.org/10.1016/j.jmapro.2025.02.003

[5] Z. Zhang, X. Lv, B. Qi, Y. Qi, M. Zhang, and Z. Tao, 'Surface roughness prediction and roughness reliability evaluation of CNC milling based on surface topography simulation', *Eksploatacja i Niezawodność – Maintenance and Reliability* 26 (2) (2024). https://doi.org/ 10.17531/ein/183558

[6] I. Danis, F. Monies, P. Lagarrigue, and N. Wojtowicz, 'Cutting forces and their modelling in plunge milling of magnesium-rare earth alloys', *Int J Adv Manuf Technol* 84 (9–12) (2016) pp. 1801–1820. https://doi.org/10.1007/s00170-015-7826-3

[7] L. Dong and M. Chen, 'A comparative experimental study on the rough machining methods of centrifugal three-dimensional impellers', *Advances in Mechanical Engineering* 16 (4) (2024). https://doi.org/10.1177/16878132241244923.

[8] Z. Cui, H. Liu, L. Wu, Z. Cao, and W. Zong, 'Cutting force and surface quality in ultra-precision milling of oxygen-free copper under different cutting strategies', *Journal of Manufacturing Processes* 131 (2024) pp. 2420–2442. https://doi.org/10.1016/j.jmapro.2024.10.056

[9] M. Płodzień, Ł. Żyłka, P. Sułkowicz, K. Żak, and S. Wojciechowski, 'High-Performance Face Milling of 42CrMo4 Steel: Influence of Entering Angle on the Measured Surface Roughness, Cutting Force and Vibration Amplitude', *Materials* 14 (9) (2021) p. 2196. https://doi.org/10.3390/ma14092196

[10] S. Wakaoka, Y. Yamane, K. Sekiya, and N. Narutaki, 'High-speed and high-accuracy plunge cutting for vertical walls', *Journal of Materials Processing Technology* 127 (2) (2002) pp. 246–250. https://doi.org/10.1016/s0924-0136(02)00151-6

[11] M. Fnides, S. Amroune, M. Slamani, A. Elhadi, M. Arslane, and M. Jawaid, 'Optimization of Manufacturing Parameters for Minimizing Vibrations and Surface Roughness in Milling Using Box–Behnken Design', *J. Vib. Eng. Technol.* 13 (1) (2025) p. 22. https://doi.org/10.1007/s42417-024-01602-x

[12] Z. Zhang, Y. Liu, Q. Han, S. Zhong, Y. Wang, and H. Liu, 'The design and cutting performance of variable pitch solid ceramic end milling tools', *International Journal of Refractory Metals and Hard Materials* 120 (2024) p. 106579. https://doi.org/ 10.1016/j.ijrmhm.2024.106579

[13] T. Cui, 'Precision Machining of Hard-to-Cut Materials: Current Status and Future Directions', *Int. J. Adv. Comput. Sci. Appl.* 15 (10) (2024) pp. 861–871 [Online]. Available: https://www.webofscience.com/wos/woscc/full-record/WOS:001348288600001

[14] F. J. G. Silva *et al.*, 'A Comparative Study of Different Milling Strategies on Productivity, Tool Wear, Surface Roughness, and Vibration', *JMMP* 8 (3) (2024) p. 115. https://doi.org/10.3390/jmmp8030115

[15] T. Dodok, N. Čuboňová, M. Císar, V. Ivanov, and D. Wiecek, 'Influence of CNC milling strategies on complex surface machining', *IOP Conf. Ser.: Mater. Sci. Eng.* 776 (1) (2020) p. 012002. https://doi.org/10.1088/1757-899X/776/1/012002

[16] T. M. Duc, N. M. Tuan, and T. T. Long, 'Optimization of Al_2 O_3 nanoparticle concentration and cutting parameters in hard milling under nanofluid MQL environment', *Advances in Mechanical Engineering* 16 (6) (2024) p. 16878132241257114. https://doi.org/ 10.1177/16878132241257114

[17] M. S. Kamer, 'The effect of cutting parameters in CNC milling on mechanical properties of 3D-printed polylactic acid tensile test samples: axis speed, cutting direction and number of cutting tool teeth', *Iran Polym J*, Feb. 2025, https://doi.org/10.1007/s13726-025-01463-5

[18] Y. Li and J. Gao, 'An Investigation of the Process Parameters Choice Criterion for Cutting Force Coefficient Identifications in Slot Milling', *IEEE Access* 12 (2024) pp. 129302–129307. https://doi.org/10.1109/ACCESS.2024.3428534

[19] M. G. Petrescu, T. Dumitru, E. Laudacescu, and M. Tănase, 'Experimental Investigation and Numerical Analysis Regarding the

Influence of Cutting Parameters on the Asphalt Milling Process', *Materials* 17 (14) (2024) Art. no. 14. https://doi.org/10.3390/ma17143475

[20] K. P. Waszczuk, 'Influence of Technological Parameters on the Cutting Temperature during Trochoidal Milling', *Manufacturing Technology* 24, (1) (2024) pp. 148–153. https://doi.org/ 10.21062/mft.2024.001

[21] F. Cai and R. Xia, 'Comprehensive Analysis of Milling Performance and Multi-Objective Parameter Optimization for YG6C Milling Tool', *Applied Sciences* 15 (1) (2025) p. 420. https://doi.org/10.3390/app15010420

[22] L. N. Liu, Z. Y. Shi, and Z. Q. Liu, 'Finite Element Modal Analysis for Face-Milling Cutter', *KEM* 589–590 (2013) pp. 19–22. https://doi.org/10.4028/www.scientific.net/KEM.589-590.19

[23] M. Reznicek and C. Horava, 'The Influence of the Choice of Machining Strategy on Production Technology', *Manufacturing Technology* 24 (1) (2024) pp. 117–130. https://doi.org/10.21062/mft.2024.014

[24] M. Al-Ahmad, A. d'Acunto, and P. Martin, 'Identification of Plunge Milling Parameters to Compare with Conventional Milling', in *Advances in Integrated Design and Manufacturing in Mechanical Engineering II*, S. Tichkiewitch, M. Tollenaere, and P. Ray, Eds., Dordrecht: Springer Netherlands 2007 pp. 461–474. https://doi.org/10.1007/978-1-4020-6761-7_31

[25] J. Varga, E. Spišák, I. Gajdoš, and P. Mulidrán, 'Comparison of Milling Strategies in the Production of Shaped Surfaces', *Adv. Sci. Technol. Res. J.* 16 (6) (2022) pp. 267–274. https://doi.org/10.12913/22998624/156817

[26] Q. Cheng *et al.*, 'Study on tool wear for efficient grooving blisk with disc milling cutter', *J Mech Sci Technol* 37 (10) (2023) pp. 5335–5348. https://doi.org/10.1007/s12206-023-0935-2

[27] X. H. Niu, L. Q. Cui, B. C. Hao, S. Y. Liu, Z. T. Zhang, and X. L. Meng, 'Analysis of Plunge Milling Force and Tool Deformation on Cr12', *AMR* 652–654 (2013) pp. 2173–2177. https://doi.org/10.4028/www.scientific.net/AMR.652-654.2173

[28] H. Chen, Z. Chen, and L. Li, 'Wear and Life of K40 Carbide Tool for Plunge Milling GH4169', *J. Phys.: Conf. Ser.* 2566 (1) (2023) p. 012058. https://doi.org/10.1088/1742-6596/2566/1/012058

[29] M. Arizmendi and A. Jiménez, 'Modelling and analysis of surface topography generated in face milling operations', *International Journal of Mechanical Sciences* 163 (2019) p. 105061. https://doi.org/10.1016/j.ijmecsci.2019.105061

[30] A. Q. Lin, M. L. Zheng, C. G. Fan, and L. Yang, 'Surface Morphology Simulation of High Speed Milled of Face Milling Cutters', *AMR* 305 (2011) pp. 225–229. https://doi.org/10.4028/www.scientific.net/AMR.305.225

[31] J. Wang, X. Qi, W. Ma, and S. Zhang, 'A high efficiency 3D surface topography model for face milling processes', *Journal of Manufacturing Processes* 107 (2023) pp. 74–87. https://doi.org/10.1016/j.jmapro.2023.10.026

[32] M. V. Roshan, C. S. Sumesh, S. S. Balaji, M. V. E. Manchi, M. U. Reddy, and A. Baghad, 'Sustainable Machining: A Case Study on Face Milling of AISI 1045 Steel Using a Multi-Objective Optimization Approach', *Int J Interact Des Manuf* 2024. https://doi.org/10.1007/s12008-024-02148-8

[33] I. Tibakh, M. A. Yallese, S. Belhadi, and M. Kaddeche, 'Multi-response optimisation during face milling of polyoxymethylene copolymer using grey relational analysis and data envelopment analysis based ranking coupled with the Taguchi approach', *Advances in Materials and Processing Technologies* (2024) pp. 1–26. https://doi.org/10.1080/2374068X.2024.2314838

[34] Z. Wang, 'The milling parameters of mechanical parts are optimized by NC machining technology', *Front. Mech. Eng.* 10 (2024) p. 1367009. https://doi.org/10.3389/fmech.2024.1367009

[35] M. Bey and Z. Tchantchane, 'Optimum Combination of Cutting Tools for Roughing Complex Parts Using Plunge Milling Machining Strategy', JM'EMP09 EMP, Bordj El Bahri, 15-16 April, 2014.

[36] S. Cafieri, F. Monies, M. Mongeau, and C. Bes, 'Plunge milling time optimization via mixed-integer nonlinear programming', *Computers and Industrial Engineering* 98 (2016) pp. 434–445. https://doi.org/10.1016/j.cie.2016.06.015

[37] Y. Cheng, J. Yang, D. Zuo, X. Song, and X. Feng, 'Tool design and cutting parameters optimisation for plunge milling blisk', *IJMR* 15 (3) (2020) p. 266. https://doi.org/ 10.1504/ijmr.2020.108192

[38] ISO 21920-2:2021(en), Geometrical product specifications (GPS) — Surface texture: Profile — Part 2: Terms, definitions and surface texture parameters. Accessed: Apr. 26, 2025. https://www.iso.org/obp/ui/en/#iso:std:iso:21920:-2:ed-1:v2:en